Proceedings of the 20th International Conference on Soil Mechanics and Geotechnical Engineering– Rahman and Jaksa (Eds)

An investigation of the geomechanical behavior of fiber-reinforced clay soil

Une étude du comportement géomécanique d'un sol argileux renforcé de fibres

Akhila Palat & Michael Hendry
Department of Civil and Environmental Engineering – University of Alberta, Edmonton, Alberta, Canada, palat@ualberta.ca

ABSTRACT: Reinforcing the soil by adding distinct fibers is an option for enhancing soil strength. Many studies were performed on fiber-reinforced sand, but studies on fiber-reinforced clay soil are limited. The research presented in this paper is an investigation into the geomechanical behavior of fiber-reinforced clay soil. Undrained triaxial compression tests are performed on soil-fiber composites to evaluate the effect of adding short, discrete fibers on the strength and pore pressure response. An optimum fiber combination (in terms of fiber content, length, and type) that results in the maximum strength of the composite is predicted. Unreinforced soil samples failed by forming a well-defined failure plane; however, fiber-reinforced samples showed a tendency to bulge. This change in behavior is attributed to the tensile stress mobilized in the fibers and the ability of fibers to distribute stresses from the potential planes of weakness to surrounding soil. Nylon fibers being hydrophilic, developed increased bonding with the soil resulting in an improvement in the maximum pore pressure developed and an increase in the deviator stress corresponding to the strain hardening region. A novel technique of preparing transparent fiber-reinforced soil is developed as a part of this study. This soil surrogate will be used to analyze the orientation of fibers within the soil and track their movement during shearing. The results of this research are anticipated to be applicable to estimate the undrained behavior and shear strength of fibrous organic soils and soils reinforced with elements that act in tension.

RÉSUMÉ : Renforcer le sol en ajoutant des fibres distinctes est une option pour améliorer la résistance du sol. De nombreuses études ont été réalisées sur du sable renforcé de fibres, mais les études sur des sols argileux renforcés de fibres sont limitées. La recherche présentée dans cet article est une enquête sur le comportement géomécanique des sols argileux renforcés de fibres. Des tests de compression triaxiale non drainés sont effectués sur des composites sol-fibres pour évaluer l'effet de l'ajout de fibres courtes et discrètes sur la résistance et la réponse à la pression interstitielle. Une combinaison optimale de fibres (en termes de teneur, de longueur et de type de fibres) qui aboutit à la résistance maximale du composite est prévue. Les échantillons de sol non renforcés ont échoué en formant un plan de rupture bien défini; cependant, les échantillons renforcés de fibres ont montré une tendance à gonfler. Ce changement de comportement est attribué à la contrainte de traction mobilisée dans les fibres et à la capacité des fibres à répartir les contraintes des plans potentiels de faiblesse vers le sol environnant. Les fibres de nylon étant hydrophiles, développent une liaison accrue avec le sol, entraînant une amélioration de la pression interstitielle maximale développée et une augmentation de la contrainte déviateur correspondant à la région de durcissement sous contrainte. Une nouvelle technique de préparation d'un sol transparent renforcé de fibres est développée dans le cadre de cette étude. Ce substitut du sol sera utilisé pour analyser l'orientation des fibres dans le sol et suivre leur mouvement pendant le cisaillement. Les résultats de cette recherche devraient être applicables pour estimer le comportement non drainé et la résistance au cisaillement des sols organiques fibreux et des sols renforcés par des éléments qui agissent en tension.

KEYWORDS: fiber-reinforcement; undrained triaxial testing; shear strength; transparent soil; fiber orientation.

1 INTRODUCTION

Previous studies on fiber-reinforced soil proved that adding randomly oriented, short, discrete fibers increases the strength, stiffness, and ductility of the composite (Maher and Ho, 1994; Zornberg and Li, 2003). The fibers behave like tension resisting elements and partially withstand the shear stress developed within the soil (Mirzababei et al. 2018). However, most of the existing studies are performed on fiber-reinforced sand and a very few have been performed on fiber-reinforced clay soil. This is mainly due to the challenges in sample preparation and the difficulty in quantifying pore water pressure and interface shear strength between soil and fibers. The objective of this study is to analyze the role of polymer fibers in altering the geomechanical behavior of clay soil. The effect of varying fiber contents, fiber lengths and types on the strength and pore pressure response of the clay soil are discussed and an optimum fiber composition is predicted.

The contribution of fibers to the strength of a soil depends on its orientation with respect to the principal axes of deformation. Fibers are in general most influential when oriented in the same direction as tensile strain, whereas the fibers under compression do not contribute any increase to the strength of the composite (Diambra et.al 2007). Assuming the fiber distribution is anisotropic in the field, the use of isotropic models will lead to inaccurate predictions of the strength gain attributed to fibers (Michalowski and Cermak, 2002). The work presented in this paper is the first comprehensive study performed to track the distribution and orientation of fibers within the clay soil. The paper also discusses a novel technique of preparing transparent fiber-reinforced soil and the ongoing work on this soil surrogate to track the movement of fibers during the different stages of testing.

2 LABORATORY TESTING METHODOLOGY

This section of the paper summarizes the laboratory testing methodology adopted as a part of this investigation.

2.1 *Materials*

The clay soil adopted in this study is EPK Kaolin manufactured by Edgar Minerals Inc. Laboratory testing of the clay soil resulted in a specific gravity of 2.4 g/cm^3, liquid limit of 58%, plastic limit of 42% and a plasticity index value of 16%. Standard proctor tests resulted in an Optimum Moisture Content (OMC) of 28% and Maximum Dry Density (MDD) of 1.5 g/cm^3. Reinforcements used are the pre- cut polypropylene (PP) fibers and nylon (PA) fibers, both supplied by MiniFIBERS. Inc, Tennessee. Synthetic fibers are chosen for this study because

their properties are controllable and pre-cut ones can be easily procured from the manufacturer. Table 1 summarizes the physical characteristics of PP and PA fibers.

Table 1. Physical properties of the synthetic fibers used in the stu dy (Technical data sheet, Minifibers, Inc).

Properties	PP	PA
Length (mm)	6, 18, 48	18
Thickness (mm)	0.035	0.035
Specific gravity (g/cm^3)	0.91	1.14
Tensile Modulus (GPa)	0.4	0.96
Moisture Absorption (%)	< 1	3.5-5.0

2.2 *Sample Preparation*

One of the most challenging aspect of this study was to prepare homogeneous fiber-reinforced soil samples for triaxial testing. The challenges faced during sample preparation and the steps taken to prepare consistent samples are described in Palat et.al. (2019).

To prepare unreinforced specimens, the required quantity of dry kaolinite clay was mixed with de-aired, distilled water at OMC in a mechanical mixer. The fiber-reinforced soil samples were prepared as two batches. Batch 1 was prepared by mixing half of the soil and half of the water using the mixer. Batch 2 was prepared by mixing the remaining half of soil, half of water and the entire fibers using the same mixer. The mixing speed and time kept constant for both batches. Batch 1 and 2 were subsequently mixed by hand. This soil lot and soil-fiber lot were sealed and stored in the moisture room for 48 hours before preparing the samples. This mix was then placed in a split mold of 50 mm diameter and 100 mm height as 5 equal layers with each layer followed by subsequent compaction. Care was taken to ensure that the compaction energy is consistent among the prepared samples. An arbor press was used to compact all samples and the number of blows were restricted to 15 per layer.

2.3 *Testing Method*

The specimen strength was measured by performing traditional Isotropic Consolidated Undrained (CU) triaxial tests, in accordance with ASTM D4767-11, Standard Test Method for Consolidated Undrained Triaxial Compression Test for Cohesive Soils. Humboldt HM-5020 load frame with a capacity of 15 kN was used for the testing. The axial load was measured by a load cell (Model No: 75/1508 by Sensotec) with a capacity of 4.5 kN and an accuracy of 0.14%. The vertical displacement of the sample was measured using a Linear Potentiometer (LP) (Model No: TR-50 by Novotechnik) with a maximum travel length of 50 mm, linearity of ± 0.075% and repeatability of ± 0.002 mm. A pressure panel was used to control the cell and backpressure applied to the sample. The pore water pressure developed within the specimen was measured by connecting a transducer at the base of the cell. The volume change in the sample during the consolidation phase was measured by attaching an automatic volume change device to the back-pressure line of the triaxial chamber. Prior to testing, the samples were saturated by applying a back pressure of 390 kPa and a cell pressure, which was slightly greater than the back pressure until a B value greater than 0.97 was achieved. The specimen was then consolidated by keeping the difference between cell pressure and back pressure equal to the desired effective stress. Following consolidation, shearing was initiated on the samples and the rate of shearing was decided based on the consolidation curves. The testing was continued until an axial strain of 20% was obtained.

2.4 *Scope of the testing program*

Seven series of CU triaxial tests were conducted as a part of this investigation. Each series included testing the samples for three different values of effective confining stresses (p_o'), 50 kPa, 100 kPa, and 200 kPa. Experimental studies were performed for three parameters which includes (a) fiber content (1%, 2%, and 3%), (b) fiber length (6 mm, 18 mm, and 48 mm), and (c) types of fibers (PP and PA). The corrections for filter paper strips and rubber membranes are not considered while calculating the deviator stress, as vertical filter paper strips were not used and the rubber membrane correction factor did not exceed 5%. Data compiled as a part of this experimental program was evaluated to determine the effect of fiber content, length and type on the strength, pore pressure response and effective stress paths of soil composites.

Table 2. Summary of the CU triaxial tests performed on unrei nforced and fiber-reinforced kaolinite clay soil.

Fiber Type	Fiber Content [%]	Fiber length [mm]	p_o' [kPa]
PP	0	0	50,100,200
PP	1	18	50,100,200
PP	2	18	50,100,200
PP	3	18	50,100,200
PP	2	6	50,100,200
PP	2	48	50,100,200
PA	2	18	50,100,200

3 RESULTS AND DISCUSSIONS

Section 3 is sub-divided into two parts. Section 3.1 discusses the role of short, discrete polymeric fibers in altering the geomechanical behavior of clay soil at three values of p_o'. The effect of varying the fiber parameters (fiber content, length, and type) on the deviator stress (q), pore water pressure (Δu), and effective stress paths in q versus mean effective stress (p') space are also discussed in this section. Section 3.2 summarizes the significance of developing an examination technique to visualize the distribution of fibers within the clay soil along with an overview of the ongoing study to track the movement of fibers.

3.1 *The role of fibers in altering the geomechanical behavior of clay soil*

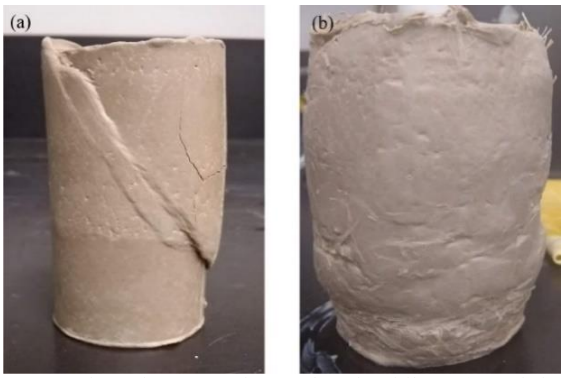

Figure 1. Deformation pattern in samples after failure (a) unreinforced sample, (b) fiber-reinforced sample (fiber content: 2 %; fiber length: 18 mm; fiber type: PP).

The effect of fiber inclusion was visually observed in all reinforced samples after shearing. The samples of unreinforced clay developed a well-defined failure plane (Fig. 1a). However, in the case of fiber-reinforced specimens, no visible failure plane

was observed, and the samples showed a tendency to bulge (Fig. 1b). The testing was stopped once an axial strain (ε_a) of 20% was reached, even though no failure was observed in the samples. This change in the mode of failure could be visualised due to the movement of fibers to the potential plane of weakness and mobilization of tension in them in the direction of expansive strain.

3.1.1 *Effect of confining pressure*

Figures 2(a) and 2(b) demonstrates the role of confining pressure on changing the peak deviator strength ($q_{\max}$) and maximum induced pore water pressure (Δu_{max}) in unreinforced and fiber-reinforced samples. For the unreinforced samples, $q_{\max}$ is taken corresponding to the peak value of q. The fiber-reinforced samples showed no signs of failure with a strain hardening response and the q at 20% ε_a is used for comparison purposes. The values of q_{max} and Δu_{max} increases with an increase in p_o' for unreinforced and all fiber-reinforced samples. In case of unreinforced samples, the particles get tightly packed at higher p_o'. This increases the bonding and force of attraction among the particles leading to an increase in the strength and pore pressure values. For fiber-reinforced samples, the increase in q_{max} and Δu_{max} with p_o' could be due to the contribution of two factors. Firstly, there will be greater interaction between soil particles and fibers leading to an increase in the frictional component of shear strength. Secondly, the amount of tension mobilized in the fibers increases with an increase in p_o' providing additional shearing resistance.

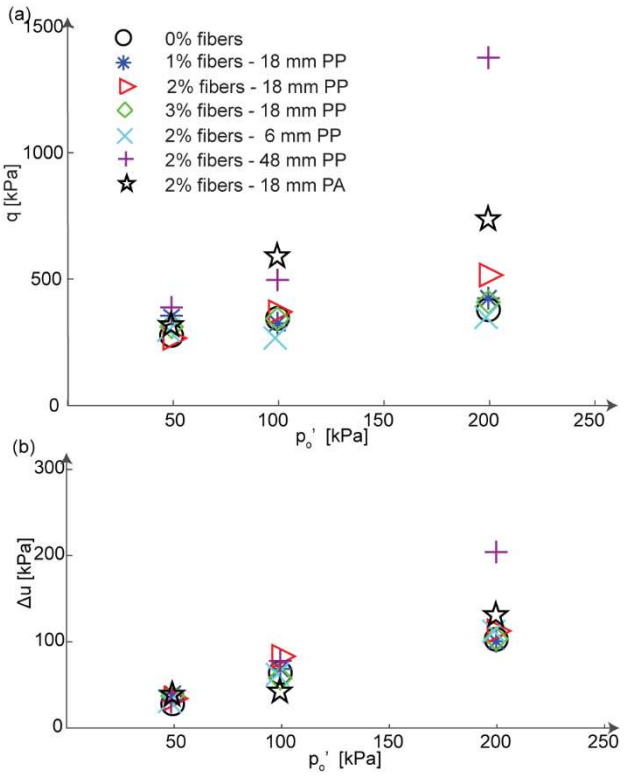

Figure 2. Results showing the effect of varying the effective confining pressure (p_o') on: (a) q and (b) Δu.

Increasing the fiber content and length have a minimal influence on the behavior of soil-fiber composite at low p_o'. The effectiveness of fibers to connect the soil particles together is less at low p_o' values. The authors would postulate a slippage of fibers during deformation rather than contributing to the shear strength of the composite. However, at higher values of p_o', the q_{max} and Δu_{max} increases on increasing the fiber content, reaches a maximum at 2%, followed by a reduction beyond this value. The highest value observed in 48 mm long fiber-reinforced composites at a p_o' of 200 kPa suggests the greater amount of tension mobilized in longer fibers. In the interpretation of authors, it appears that the geotechnical structures subjected to higher confining pressure would benefit significantly from reinforcing with longer fibers.

3.1.2 *Effect of fiber content*

Figures 3(a), 3(b), and 3(c) shows the CU triaxial test results for samples reinforced with different fiber contents and consolidated at a p_o' of 200 kPa. The fiber length kept constant as 18 mm. The response of the fiber-reinforced specimen at other values of p_o' can be provided if required.

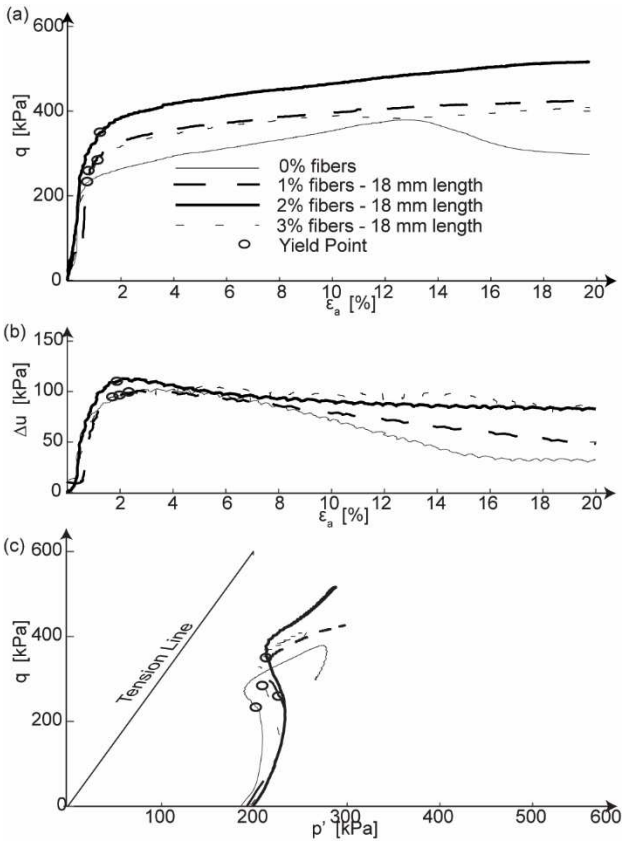

Figure 3. Results showing the effect of varying the fiber content (fiber length: 18 mm; fiber type: PP) on: (a) q versus ε_a (b) Δu versus ε_a (c) q versus p', at a p_o' of 200 kPa.

The unreinforced clay samples demonstrated a strain weakening behavior after the attainment of q_{max}. However, the samples of fiber-reinforced clay showed a strain hardening behavior past the yield point. This linear increase in q corresponding to the strain-hardening region is entirely due to the tensile forces developed in the fibers (Hendry et al., 2012). It is also an indication of the improvement in the ductility of clay soil by the inclusion of randomly oriented fibers. The q and Δu_{max} increases on increasing the fiber content, reaches a maximum at 2%, followed by a reduction beyond this value. This reduction in the strength beyond the threshold value (2%) could be due to the tendency of fibers to get clustered inside the soil sample rather than being distributed uniformly. Shearing develops among individual fibers leading to a reduction in the strength and pore pressure response on increasing the fiber content beyond this optimum value of 2%. A similar trend was also observed in the shear strength response of fiber-reinforced sand (Zornberg et al., 2004). The reason for this behavior could be due to the different types of soil reinforcement mechanisms developed within the soil-fiber composite. Initially, tensile forces develop in the fibers

leading to an increased overall shear strength of the matrix. At higher values of fiber contents (greater than the optimum), shear among individual fibers becomes the governing factor, leading to a reduction in the shear strength values. The q versus p' indicate a strain hardening response with maximum q value observed for 2% fiber-reinforced samples. However, none of them has traced the path of the tension cut-off line, which indicates that the maximum tension has not mobilized in the fibers.

3.1.3 *Effect of fiber length*

Figures 4(a), 4(b), and 4(c) shows the q versus ε_a, Δu versus ε_a, and q versus p' plots when reinforced with three different lengths of PP fibers (6 mm, 18 mm, and 48 mm) and tested at a p_o' of 200 kPa. The fiber content kept constant at 2%. All samples exhibited a strain hardening behavior after yielding and a bulging mode of failure without any evidence of failure plane.

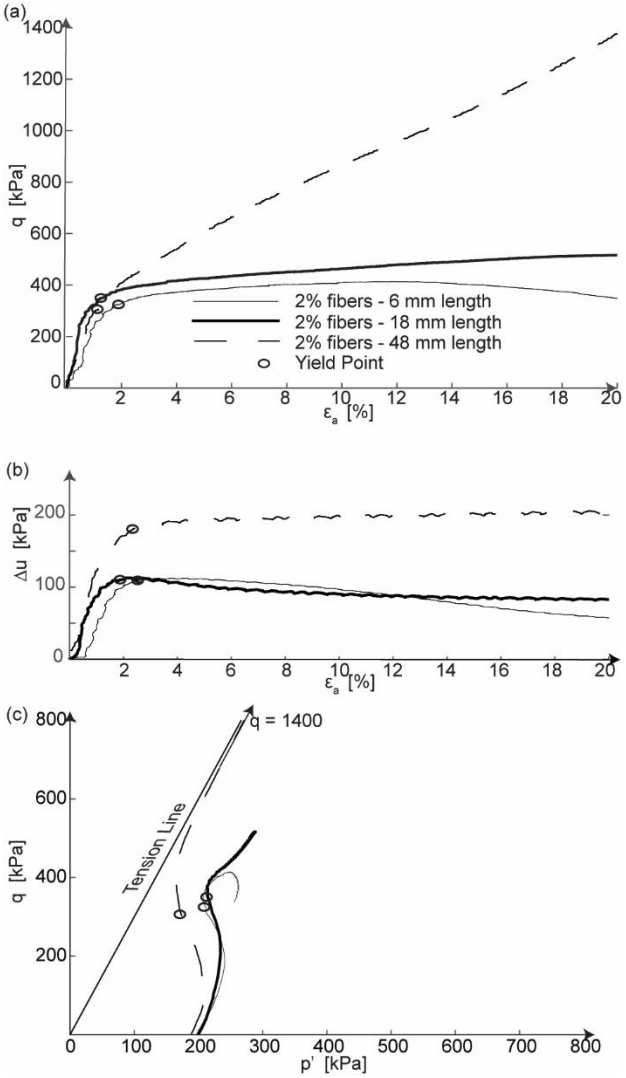

Figure 4. Results showing the effect of varying the fiber length (fiber content: 2%; fiber type: PP) on: (a) q versus ε_a (b) Δu versus ε_a (c) q versus p', at a p_o' of 200 kPa.

For the range of fiber lengths adopted in this study, the q_{max} and Δu_{max} increased on increasing the fiber length from 6 mm to 48 mm. One potential reason for this trend could be the greater area of contact between fibers and soil leading to an increase in the frictional component of shear strength. Additionally, increasing the fiber length improves the pullout resistance of individual fibers (Zornberg et al., 2004). This in turn leads to the mobilization of tensile forces within the fibers, which would also contribute to the overall shear strength of the matrix. It can be predicted that the optimal fiber length for use in practice is beyond the range of lengths that the author has tested. For 48 mm long fiber-reinforced samples, the q versus p' plot (Fig. 4c) follows the trace of tension cut-off line. This is an indication that the maximum tensile strength has been mobilized in the fibers. However, on examining the samples after failure, the fibers did not show any tendency of breakage. The tensile modulus of the PP fiber is 0.4 GPa (Table 1). This concludes that the fibers are highly extensible and the force required to break them were not reached during the triaxial testing.

3.1.4 *Effect of fiber type*

Two different types of synthetic fibers are used in this study, PP and PA. The fiber content and length kept constant at 2% and 18 mm respectively. The q versus ε_a, Δu versus ε_a and q versus p' response are illustrated in Fig. 5a, 5b, and 5c.

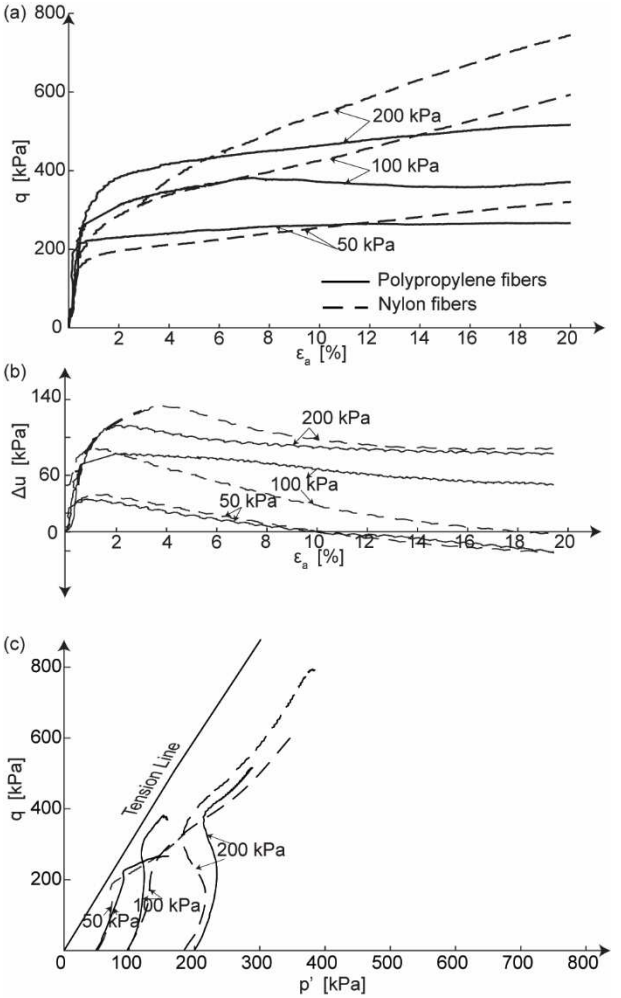

Figure 5. Results showing the effect of varying the fiber type (fiber content: 2%; fiber length: 18 mm) on (a) q versus ε_a (b) Δu versus ε_a (c) q versus p', at three values of p_o'.

Both fibers have contributed to an increase in the strength and pore pressure response compared to an unreinforced soil sample. The initial portion of the stress-strain curves are similar for both fibers, which implies that the fiber type has a minimal influence on the vertical stiffness (E_V) of the composite. However, PA fibers show better strain hardening and higher Δu_{max} compared to PP fibers. The same method of sample preparation was adopted for preparing PA and PP fiber-reinforced soil samples. Therefore, this change in the response could be because of the difference in the affinity of these fibers to water. The

moisture absorption capacity of PP fiber is less than 1% while it ranges from 3.5% - 5% for PA fibers (Table 1). PA being hydrophilic has increased bonding with the soil-water mix compared to the hydrophobic PP fibers. The authors speculate that the increased adhesion and bonding of PA fibers with water outweigh the differences in surface texture resulting in a change in response between the fiber types.

3.2 *Visualization techniques to track the fiber distribution*

The absence of failure plane in fiber-reinforced sample is presumed due to the movement of fibers to the potential planes of weakness and mobilization of tensile forces. Additionally, the linear increase in q during strain hardening is expected due to the additional shear resistance developed because of fiber tension (Hendry et al., 2012). This could also be visualized as a reorientation of fibers in the horizontal direction (direction of expansive strain) during shearing and mobilization of tensile stresses in them (Palat et.al, 2019). Fibers have also proved to exhibit a bridging effect thereby impeding the development of tension cracks in the clay soil (Tang et.al, 2007). All justifications to these observed trends during laboratory testing of fiber-reinforced samples are based on the judgement of the researcher; hence, several ambiguities exists about these predictions. Through this study, the authors are working on developing an examination technique to visualize the distribution and orientation of fibers within the clay soil and track their movement during shearing.

Figure 6. Samples of fiber-reinforced clay (2%-18 mm PP fibers) after failure (a) wet sample, (b) dry sample.

Several methods were tried out as a part of this investigation. The samples were initially sheared to failure followed by the visual examination by cutting a plane through the specimen. Figure 6(a) and 6(b) shows the wet and dry images of a fiber-reinforced soil sample after subjecting to failure. It is obvious from the images that the predominant orientation of fibers is horizontal. On possible reason for this behavior, could be due to the higher compaction energy imparted using the arbor press during sample preparation. Additionally, there would also be a tendency for a few fibers to realign in the horizontal direction due to the pressure imparted to the sample while cutting. However, visually counting the number of fibers intersecting a plane is not feasible due to the lower diameter of polypropylene fibers and the optimum fiber content used in the sample preparation (2%) is a way higher than the maximum adoptable fiber content (0.25%) specified in the previous studies. (Diambra et.al, 2007, Ibrahim et.al, 2012).

Fiber reinforced samples were subjected to Computerized Tomography (CT) scans and the images were analyzed to examine the orientation of fibers in the specimen. The Toshiba Aquilion One X-Ray CT Scanner available at the research park facility of Alberta Innovates was used for scanning the fiber-reinforced samples. This 320-slice helical scanner had a resolution of 300 micrometers and used an energy of 100 kV for the X-Ray scan beam. Figure 7(a) shows the negative of a Digital Imaging and Communications in Medicine (DICOM) image representing a slice of thickness 300μm as retrieved from the CT scan. Detecting the presence of polypropylene fibers out of the DICOM image was a great challenge owing to the difficulty of fibers in interacting with the X-Ray energy due to their low-density value. Subsequently a program was developed in Matlab by adopting the principle of Canny Edge detection algorithm (Fisher et.al, 1996) to detect the lines in each DICOM image. However, the lines in the final image retrieved from Matlab (Fig 7(b)) represents the air and water boundaries, along with the fibers.

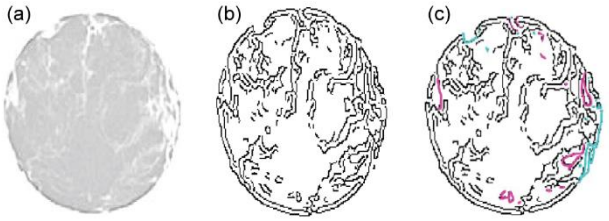

Figure 7. Procedure for determining the fibers out of a CT scanned image (a) DICOM slice, (b) Final image from Matlab, (c) Image after filtering out the fibers from the air and water boundaries.

The grayscales in the DICOM images reflect the relative linear attenuation coefficient (μ) of the components, which determines the degree to which different components are distinguishable. The value of μ for air and water are -1000 Hounsfield Unit (HU) and 0 HU respectively. By using the software Image J (that is adopted for determining the μ value in a DICOM image), air and water boundaries were filtered out from the eventual Matlab image. Figure 7(c) shows the final output where black lines indicate fibers, pink lines indicate the pore air spaces and blue line shows the pore water spaces. However, adopting the technique of CT scanning for detecting the fibers is time consuming, as it is required to apply canny edge detection principle to each individual slice and filter out fibers from the air/water boundaries. In addition, CT scanning of the samples is expensive and requires knowledge of the complex equipment used. Due to these constrains, the authors are now working on developing a fiber-reinforced transparent soil to visually examine the orientation of fibers in the soil and track their movement during testing.

Transparent soil is developed when a soil is saturated with a fluid of matched refractive index. Owing to the same refractive index, the soil/fluid combination appears homogeneous to light and becomes transparent (Iskander, 2002). For this study, the transparent clay soil is develop by using the pyrogenic fumed silica HDK H18 supplied by Wacker products along with a combination of Purity FG white oil and Paraflex HT4 process oil, both supplied by Petro Canada. The silica powder to pore fluid ratio kept constant at 6:94. The density of silica particles, white oil and process oil are 2.2 g/cc, 0.86 g/cc and 0.82 g/cc respectively. For preparing the specimen, the white oil and process oil were mixed in the volumetric proportions of 77:23 using a hand held food mixer. Fumed silica powder (6% by weight of the total pore fluid combination) was added to this pore fluid mix and mixed vigorously until a transparent gel is formed. The soil-pore fluid mixture was then transferred to a vacuum chamber to de-air the solution. This de-aired mix was transferred to a cylindrical mold and fibers (2% by weight) were mixed uniformly in the solution. Figure 8. shows the fiber-reinforced transparent soil prepared as a part of this investigation.

Figure 8: The fiber-reinforced transparent soil prepared as a part of this investigation.

This is an ongoing study wherein the images of fiber-reinforced transparent soil are taken with a Canon EOS Rebel T7i digital camera which is triggered every 30 minutes using the EOS utility software installed in a computer. The images are then processed to track the movement of fibers during the consolidation of the slurry. The study also aims at performing triaxial tests on samples cut from the slurry to observe the movement of fibers during shearing.

4 CONCLUSIONS

Adding randomly oriented, short, discrete fibers is an effective technique for improving the strength and stability of clay soil. On par with being used as a ground modification technique, the fiber-reinforced clay soil can also be used in several other applications such as evapotranspiration covers, oil sands mining reclamation, including tailings pond, low-permeable landfill liners, etc. This study is an investigation of the geomechanical behavior of fiber-reinforced clay soil. The variables used in the testing program are confining pressure, fiber content, lengths and types of fibers. The fiber-reinforced clay samples exhibited a strain hardening behavior with no signs of failure; hence, it was not possible to define the shear strength for this material. The major observations from this study are summarized below:

- The unreinforced clay samples exhibited a well-defined failure plane and demonstrated a strain weakening behavior after the attainment of q_{max}. However, reinforced samples showed a tendency to bulge without any evidence of failure plane. This is an indication of the improvement in the ductility of the clay soil by the addition of fibers. Resistance to cracking potential accompanies an improvement in the ductility and is beneficial while using this composite as landfill liners or evapotranspiration covers.
- The q and Δu_{max} increases with an increase in the fiber content, up to an optimum amount of 2%, followed by a reduction with further increase. On increasing the fiber content beyond 2%, the fibers develop a tendency to cluster inside the soil rather than distributing uniformly. The shear among the individual fibers becomes the dominating mechanism and the contribution of mobilized fiber tension to the overall shear strength of the composite reduces.
- For the range of fiber lengths used in this study, the q and Δu_{max} increases with an increase in the length of fibers. This is due to the greater area of contact between fibers and soil resulting in a higher interface shear strength and the greater amount of tension mobilized in longer fibers. This concludes that the optimal fiber length for use in practice is beyond the range of lengths the author has tested.
- PA fiber-reinforced clay soil showed better strain hardening and higher Δu_{max} compared to PP fiber-reinforced samples. This could be because of the difference in the affinity between the fibers and soil-water mix as PA is hydrophilic, and PP is hydrophobic.
- The orientation of fibers in the soil plays a crucial role in determining the strength of the soil-fiber composite. Three different techniques are discussed in this paper to analyze the distribution of fibers within the clay soil and track their movement during consolidation and shearing.
- A novel technique of preparing transparent fiber-reinforced soil is proposed as a part of this study. This soil surrogate will be used in the future to analyze the orientation of fibers within the soil and track their movement during consolidation and shearing.

5 ACKNOWLEDGEMENT

This research is funded by a Natural Sciences and Engineering Research Council Discovery Grant (RGPIN-2020-04419). The authors also like to thank MiniFIBERS. Inc, for supplying the fibers for testing.

6 REFERENCES

Acharya, M.P. Hendry, M.T. and Martin, C.D. 2017. Creep behaviour of remoulded and intact fibrous peat. Acta Geotechnica, 13(2): 399–417.

Diambra, A. Russel, A. R. Ibrahim, E and Wood, D.M. 2007. Determination of fiber orientation distribution in reinforced sands. Geotechnique 57, No. 7, 623–628, doi: 10.1680/geot.2007.57.7.623.

Fisher, R. Perkins, S. Walker, A. and Wolfart, E. 2000. Hypermedia Image Processing Reference. JOHN WILEY & SONS LTD.

Hendry, M, T. Sharma, J, S. Martin, C, D. and Barbour, S, L. 2012. Effect of fibre content and structure on anisotropic elastic stiffness and shear strength of peat. Canadian Geotechnical Journal 49: 403–415.

Hendry, M.T. Martin, C.D. & Barbour, S.L. 2013. The measurement of the cyclic response of railway embankments and underlying soft peat foundations to heavy axle loads. Can. Geotech. J., 50(5), 467-480.

Hendry, M.T. Barbour, S.L. and Martin, C.D. 2014. Evaluation of the effect of fibre reinforcement on the anisotropic undrained stiffness and strength of peat. ASCE J. Geotech. Geoenviron. Eng., 140(9).

Ibrahim, E. Diambra, A. Russel, A. R. and Wood, D.M. 2012. Assessment of laboratory sample preparation for fibre reinforced sands. Geotextiles and Geomembranes, Volume 34, October 2012, pages 69-79.

Iskander, M. Liu, J. and Sadek, S.2002. Transparent amorphous silica to model clay. Journal of geotechnical and geoenvironmental engineering. DOI: 10.1061/ (ASCE)1090-0241(2002)128:3(262).

Maher, M, H. and Ho, Y, C. 1994. Mechanical properties of kaolinite/fiber soil composite. Journal of Geotechnical Engineering, 120(8): 1381-1393.

Michalowski, R.L., and Čermák, J. 2002. Strength anisotropy of fiber-reinforced sand. Computers and Geotechnics, 29(4): 279– 299. doi:10.1016/S0266-352X(01)00032-5.

Mirzababaei, M. Mohamed, M. Arulrajah, A. Horpibulsuk, S and Anggraini, V. 2018. Practical approach to predict the shear strength of fiber-reinforced clay. Geosynthetics International, 25, No.1.

Palat, A. Hendry, M.T. Roustaei, M. 2019. Effect of fiber content on the mechanical behavior of fiber-reinforced clay. In Proceedings of the 72nd Canadian Geotechnical Society Annual Conference, GeoStJohns 2019, StJohns, Newfoundland. 29 September - 2 October 2019.

Tang, C. Shi, B. Gao, W. Chen, F. and Cai, Y. 2007. Strength and mechanical behavior of short polypropylene fiber reinforced, and cement stabilized clayey soil. Geotextiles and Geomembranes, 25 (3), 194–202.

Zornberg, J.G. Cabral, A.R and Viratjandr, C. 2004. Behavior of tire shred – sand mixtures. Canadian Geotechnical Journal, 41,227-241, doi: 10.1139/T03-086.

Zornberg, J.G. and Li, C. 2003. Design of Fiber-Reinforced Soil. In Proceedings of the Twelfth Panamerican Conference of Soil Mechanics and Geotechnical Engineering, Cambridge, Massachusetts, June 22-26 Vol. 2, pp. 2193-2200.